

4. A Fuzzy Classification Technique Applied to Fault Diagnosis

Cosmin Danut Bocaniala and José Sá da Costa

This chapter describes a novel fuzzy classification methodology for fault diagnosis. There are three main directions of applying fuzzy classifiers to fault diagnosis: neuro-fuzzy classifiers, classifiers based on collections of fuzzy rules, and classifiers based on collections of fuzzy subsets. The contributed fuzzy classification methodology described in this chapter follows the last direction. The main advantages of the developed fuzzy classifier are the high accuracy with which it delimits the areas corresponding to different system states, i.e., the normal state and the different faulty states, and the fine precision of discrimination inside overlapping areas. In addition, the classifier needs to tune only a small numbers of parameters, i.e., the number of parameters equals the number of system states considered. The methodology is validated by application with very good results to fault diagnosis of a control flow valve from an industrial device.

4.1. Introduction

The goal of fault diagnosis research is improving the security, efficiency, maintainability and reliability of industrial plants. There are two main types of systems that are addressed: safety-critical systems such as nuclear plants and aircraft, and lower safety-critical systems such as process and manufacturing plants. A fault diagnosis system is a monitoring system that is used to detect faults and diagnose their location and significance in a system (Chen and Patton, 1999). The diagnosis system performs mainly the following tasks: fault detection – to indicate if a fault occurred or not in the system, and fault isolation – to determine the location of the fault.

According to Duda and Hart (1973), classification represents “the assignment of a physical object or event to one of several prespecified categories.” Fault diagnosis represents a suitable application field for classification methods, as its main purpose is to achieve an optimal mapping of the current state of the monitored systems into a prespecified set of system states. The set of system states includes the normal state and the faulty states (Ariton and Palade, 2005). A general framework for applying classification methods to fault diagnosis problems is given in (Leonhardt and Ayoubi, 1997). Fault diagnosis is described as “a sequential process involving two steps: the symptoms extraction and the actual diagnostic task.” The symptoms are extracted on the basis of the measurements provided by the actuators and sensors in the monitored system. The actual diagnostic task is to map the points in the symptoms space into the set of considered faults. For this

reason, the use of classification techniques represents a natural choice when designing a fault diagnosis system.

There are three main ways for applying fuzzy classifiers to fault diagnosis that can be found in the literature. Fault diagnosis may be performed using collections of fuzzy rules (Frank, 1996; Koscielny *et al.*, 1999). Let $R = \{r_1, r_2, \dots, r_m\}$ be the set of residuals. Each residual r_i , $i=1, \dots, m$, is described by a number of fuzzy sets $\{r_{i1}, r_{i2}, \dots, r_{is}\}$. The causal relationships between the residuals and faults are expressed by if-then rules having a form similar to

$$IF (effect = r_{ip}) AND (effect = r_{jq})... THEN (cause is the k - th fault) \quad (1)$$

The output of the fuzzy classifier is the faulty vector F . The fuzzy inference process will assign to each component F_i , $i=0, 1, \dots, n$, where n is the number of faults – a value between 0 and 1 that indicates the degree with which the normal state (the corresponding component is F_0) or the j -th fault affects the monitored system, $j=1, \dots, m$. If there is the premise that the system can be affected only by a fault at a time, then the faulty vector contains only one component larger than a preset threshold value, and whose corresponding faulty state represents the actual state of the monitored system. If multiple faults can affect the monitored system, then the components of the classifier output, which are larger than a preset threshold, indicate the faults that occurred in the system. The main advantage of using sets of fuzzy rules is that they make transparent the relationships between symptoms and faults via the use of linguistic terms. However, notice that if the number of fuzzy sets used is increasing, the number of linguistic terms used to label them also increases. It follows that the linguistic informational burden of the operator may increase too beyond reasonable limits.

Combinations between fuzzy logic and neural networks, i.e., neuro-fuzzy systems, are used to create diagnosis systems robust to uncertainties and noise (Palade *et al.*, 2002; Uppal *et al.*, 2002). Calado *et al.* (2001) propose a hierarchical structure of several fuzzy-neural networks (FNN) for fault isolation purposes. The hierarchical structure has three levels. The first order differences for all available measurements are used as symptoms. The lower level consists of one FNN that receives as input the considered symptoms. The output of this FNN determines which of the FNNs on the medium level will be activated. That is, if the i -th component of the output has a value close to 1, then the i -th FNN on the medium level will be activated. The number of the FNNs on the medium level is equal to the number of faults considered. Each one of them is also fed with all symptoms considered. The upper level is used to perform an OR operation on the outputs of the activated FNNs on the medium level. The components of the outputs considered for the OR operation must have a value close to 1. The main advantage of the neuro-fuzzy systems is that the learning, adaptation and parallelism capabilities provided by neural networks may be used to tune the fuzzy rules parameters. The main drawback of the neuro-fuzzy classifiers, like the one presented before, is represented by a possible too large number of parameters to be tuned, i.e., fuzzy membership functions and neural network weights.

A third direction is to represent the normal state and each faulty state of the system as a fuzzy subset of the symptoms space (Boudaoud and Masson, 2000). The quality of this last direction is given by its capabilities to learn the topological structure of the space. Boudaoud and Masson (2000) propose two main steps for the

design of such a pattern recognition diagnosis system: analysis and exploitation. The analysis phase is performed off-line and it transforms the available measurements, labelled with the corresponding operating state of the system, into a collection of fuzzy subsets standing for regions in the measurements space describing the operating states into the measurements space. The exploitation phase corresponds to the on-line diagnosis process using classification into the regions found before.

The fuzzy subsets defining the normal state and the faulty states of the system represent hyperboxes B defined by a minimum point m and a maximum point M in the symptoms space (Boudaoud and Masson, 1996). Figure 4.1 shows a hyperbox in \mathbb{R}^3 . This type of fuzzy subsets has been used with the fuzzy min-max clustering algorithm proposed by Simpson (1993). The maximal size of each hyperbox is tuned so that the misclassification rate is minimal. The particularities of the fuzzy subsets defined by hyperboxes, i.e., full membership inside hyperboxes and partial membership around hyperboxes boundaries, allow diagnosis to consist of three possible cases: (i) the system state is stationary, (ii) the system is in transition between two possible states, and (iii) the system is stabilizing in a new state. It is important to mention that the hyperboxes used during the diagnosis process are not allowed to overlap (Simpson, 1993). This does not mean that the areas in the symptoms space corresponding to different states do not overlap, but that the hyperboxes delimit the sub areas where points have full membership. Diagnosing the partial membership areas as transitions between two states compensates the loss of diagnosis information due to this approach.

Notice that the dimension of each hyperbox depends on only three constraints: its minimum point, its maximum point, and a parameter that controls the decreasing rate of membership to B value when the distance between a test point u and B increases. Thus, the main advantage of the third direction compared to the previous two directions is the smaller number of parameters to be tuned, i.e., three times the number of system states considered, which leads to a smaller designing time for the classifier. However, the transparency of relationships between symptoms and faults given by the use of linguistic terms is lost.

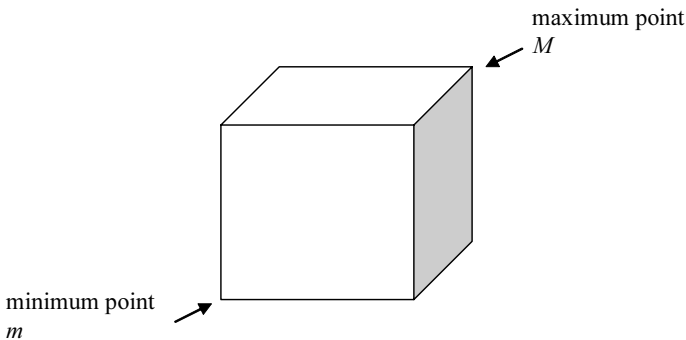


Figure 4.1. A hyperbox in \mathbb{R}^3 defined by minimum and maximum points.

The classification methodology described in this chapter follows the last direction mentioned. The methodology is described in detail in our previous papers (Bocaniala *et al.*, 2004; 2005). The main property of this methodology is the large accuracy with which it learns the topological structure of the symptoms space. The fuzzy subsets built by the classifier approximate with a very small error the areas in the symptoms space corresponding to different system states. Its accuracy also manifests through handling with fine precision the discrimination inside overlapping areas.

The fuzzy subsets defined by this methodology express better the topological properties of the symptoms space than hyperboxes used in (Boudaoud and Masson, 1996). Details are given further in the chapter. Also, similar to the methodology proposed in (Boudaoud and Masson, 1996), the methodology in this chapter also needs to tune only a small numbers of parameters, i.e., the number of parameters equals the number of system states considered. Details are given further in the chapter as well.

The chapter is organized as follows. Section 4.2 presents the theoretical aspects of the described fuzzy classification methodology. The case study, DAMADICS benchmark (<http://www.eng.hull.ac.uk/research/control/damadics1.htm>), is concerned with fault diagnosis of a valve intended to supply water to a steam generator boiler. Section 4.3 provides a detailed analysis of the faults studied by the benchmark. Section 4.4 presents the detection and isolation of the valve faults using the contributed fuzzy classifier. Section 4.5 summarizes the original contributions of this chapter and mentions possible directions for future work.

4.2. Theoretical Aspects of the Contributed Fuzzy Classification Methodology

The fuzzy subsets used by the classification methodology described in this chapter are induced (built) on the basis of a point-to-set similarity measure between a point and a set of points in the measurements space (Baker, 1978). The point-to-set similarity is built at its turn on the basis of a point-to-point similarity measure between points in the measurements space.

One of the particularities of the methodology is the fact that one may choose those point-to-point and point-to-set similarities that provide the best classification performance for the problem at hand. Thus, the methodology may be seen as a template that may be instantiated so that it fits the specific characteristics of the problem to solve. One may criticize this aspect as it implies searching by trials the most suitable similarity measures. However, hints on what measures should be used may be obtained by analysis of the measurements used. For instance, the trends in the available sensor measurements may reflect in the same way the effects of a fault on a system. Therefore, the use of a measure of similarity between the trends in the sensor signals over a time window may prove to be a good choice.

In order to facilitate the understanding of the theoretical concepts presented in the following, a simple problem shown in Figure 4.2 is used. The

figure shows the points corresponding to two categories characterized by two measurements.

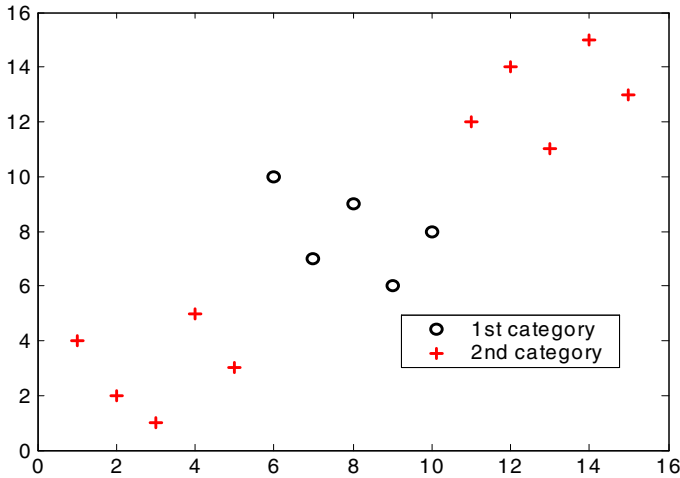


Figure 4.2. The simple problem used to illustrate the theoretical aspects.

4.2.1. Point-to-Point Similarity Measure Based on Distance Functions

The similarity between two points u and v , $s(u,v)$, may be expressed using a complementary function, $d(u,v)$, expressing dissimilarity. Baker (1978) expresses dissimilarity by using the distance function in Eq. 2. Notice that, in this case, the functions s and d are complementary with regard to unit value, $s(u,v)=1-d(u,v)$. The β parameter plays the role of a threshold value for the similarity measure. For a data point u , all points v residing at a distance $\delta(u,v)$ smaller than β will bear some similarity with u . As for the points residing at distances larger than or equal to β , the similarity $s(u,v)$ is null. The contour plot of the point-to-point similarity function when Eq. 2 is used is shown in Figure 4.3. The distance measure used is the Euclidean measure.

$$h^\beta(\delta(u,v)) = \begin{cases} \delta(u,v)/\beta, & \text{for } \delta(u,v) \leq \beta \\ 1, & \text{otherwise} \end{cases} \quad (2)$$

4.2.2. Point-to-Point Similarity Measure Based on Pearson Correlation

The Pearson correlation (Weisstein, 1999) measures the similarity in the trends of two signals. Let us suppose that s and t represent the measurements of two signals over the same time window. The formula used to compute the correlation between the vectors s and t is given in Eq. 3. The terms z_s and z_t represent the z -scores of s

and t , respectively. The z -score of a vector is obtained by first subtracting the mean value and then dividing by its standard deviation. The product between zs and zt is the dot product and n represents the length of the time window.

$$p(s, t) = 1 - (zs \cdot zt) / n \tag{3}$$

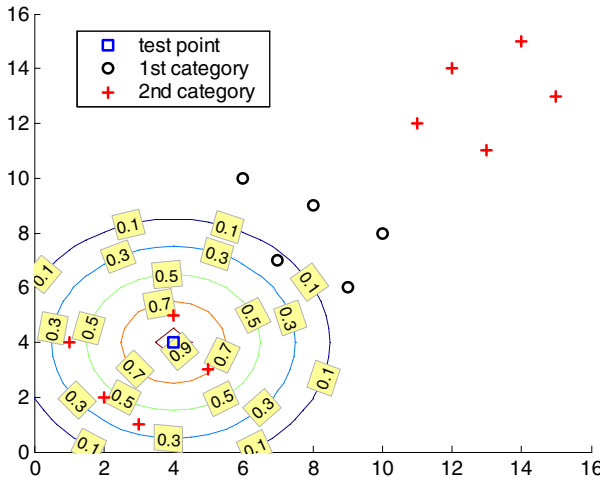


Figure 4.3. The point-to-point similarity measure for $\beta=5$ in Eq. 2.

The values of this correlation measure fall in $[0,2]$ interval, where 0 stands for perfect correlation and 2 stands for perfect anticorrelation. Figure 4.4 shows two pairs of shapes corresponding to these two cases. There is a parallel between the terms “correlation”/“anticorrelation” and the terms “similarity”/“dissimilarity.” Indeed, the function p may play the same role as the dissimilarity function d in the previous subsection. In this case, the maximum value for $d(s,t)$, which is equal to $p(s,t)$, is 2. The functions s and d are complementary with regard to this value; thus, $s(u,v)=2-d(u,v)$.

4.2.3. Point-to-Set Similarity Measure

The similarity measure between two data points may be extended to a similarity measure between a point and a set of points (Baker, 1978). In this chapter, if the point-to-point similarity is given by Eq. 2, the similarity between a given point u and a set of points S is computed as the mean value of the point-to-point similarity values between u and each v in S (Eq. 4, where n denotes the number of elements in S). Notice that the value of $r(u,S)$ stays inside $[0,1]$ interval, as $s(u,v)$ also stays inside $[0,1]$ interval and the cardinal of S is n .

$$r(u, S) = \frac{\sum_{v \in S} s(u, v)}{n} \tag{4}$$

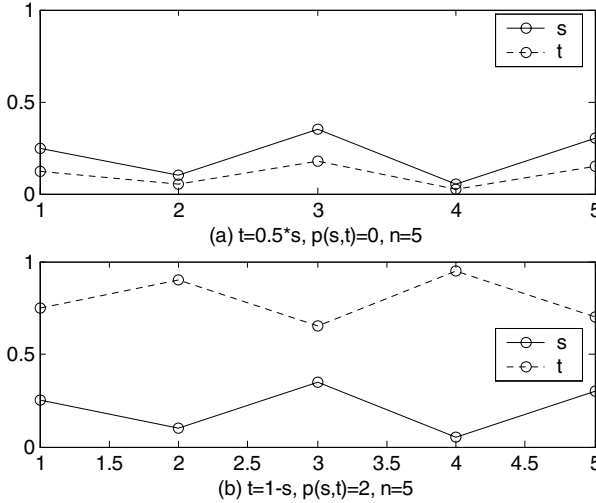


Figure 4.4. Perfect Pearson correlation (a) and perfect Pearson anticorrelation (b).

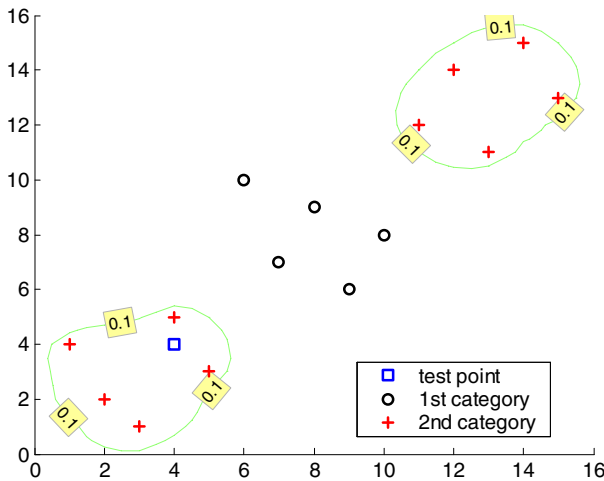


Figure 4.5. The contour plot of the point-to-set similarity for the first category ($\beta=3$).

The effect of using the β parameter is that only those data points from S , whose distance to u is larger than β , contribute to the point-to-set similarity value. The explanation is that only these points have a nonzero similarity with u . It follows that the similarity value between u and S is decided within the neighborhood defined by β .

It has been observed in practice that, if different (dedicated) β parameters are used for different categories to express the point-to-point similarity (Eq. 2), the performance of the classifier increases substantially. Let us consider that the value of the β parameter is 3 for both categories in the problem. The contour plots of the

point-to-set similarity functions for the two categories are shown in Figures 4.5 and 4.6 (left), respectively. The two plots are drawn for all the points in the Cartesian product $[0,16] \times [0,16]$. If we decrease the value of β to 1.8 for the second category, the contour plot for this category matches more accurately the topology of the area occupied by points in the category (Figure 4.6, right).

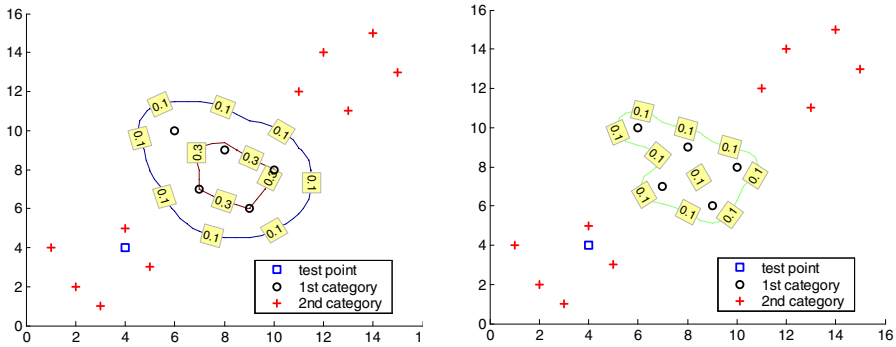


Figure 4.6. The contour plot of the point-to-set similarity for the second category when $\beta=3$ (left) and when $\beta=1.8$ (right)

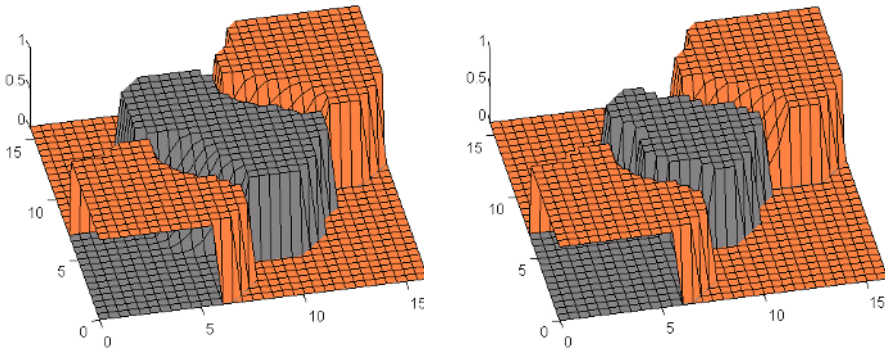


Figure 4.7. The surfaces generated when the same β value is used (left) and when different β values are used (right)

4.2.4. Fuzzy Subsets Induced by Single Point-to-Set Similarity Measures

Let $C = \{C_i\}_{i=1, \dots, m}$ be the set of all points in the measurements space, associated with the problem to solve, where C_i , $i=1, \dots, m$, represents the set of all points corresponding to the i -th considered category. The membership function of the fuzzy subset $Fuzz_i$ induced by C_i , computed on the basis of a given point-to-set similarity measure, is given in Eq. 5. The n value represents the cardinal of C , and the n_i value represents the cardinal of C_i .

$$\mu_i(u) = \frac{r(u, C_i)}{r(u, C)} \quad (5)$$

If the values of the β parameters considered are the same: 3 for both categories, the obtained fuzzy subsets (surfaces) corresponding to the two categories are shown in Figure 4.7 (left). If different values for the β parameters are used: 3 for the first one and 1.8 for the second one, the surface corresponding to the second category shrinks to match better the topology of the area occupied by the points in that category (Figure 4.7, right).

A point u presented at the input of the classifier is assigned to the category C_z whose corresponding degree of assignment $\mu_z(u)$ is the largest (Eq. 6). In case of ties, the assignment to a category cannot be decided and the point is rejected.

$$u \in z\text{-th category} \Leftrightarrow \mu_z(u) = \max_{i=1, \dots, m} \mu_i(u) \quad (6)$$

4.2.5. Fuzzy Subsets Induced by Multiple Point-to-Set Similarity Measures

The practice showed that there are problems for which classifiers designed by using only one point-to-set similarity measure does not provide satisfactory results (Bocaniala *et al.*, 2004). When situations like these are met, the advantages brought by two or more similarity measures may be combined in order to improve the performance of the classifier (Bocaniala *e. al.*, 2004), i.e., a hybrid approach is used. This aspect has also been noticed by Baker (1978).

In the following, a few possible approaches, when trying to combine the use of two or more similarity measures, are suggested:

- similarity measures: the β parameter may be applied only to one of the similarity measures used; if more than one similarity measure is used, then there is a β parameter for each one of them.
- cluster affinity measures: there may be only one cluster affinity measure resulting from the combination of all similarities used; or, there may be one cluster affinity measure for each similarity used.
- fuzzy membership functions: the fuzzy membership functions represent combinations of cluster affinity measures if more than one such measure exists.

If the β parameter is applied to only one of the similarity measures used, then all other cluster affinity measures will be computed for the neighbourhood defined by this β parameter.

In this chapter, a hybrid approach based on Euclidean distance and Pearson correlation is used. For details see the case study in Section 4.3.

4.2.6. Designing and Testing the Classifier

Let m be the number of the categories considered for the problem to be solved. The proposed methodology first groups the set of all available data C into clusters according to the category they belong to, C_i , $i=1, \dots, m$. In order to design and test

the classifier, each subgroup C_i is split in three representative and distinct subsets, C_i^{ref} , C_i^{param} , and C_i^{test} . On the basis of these subsets three sets unions, REF , $PARAM$ and $TEST$, are defined (Eq. 7). They are called the *reference patterns* set, the *parameters tuning* set, and the *test* set, respectively. A subset is considered representative for a given set if it covers that set in a satisfactory manner. In the following, the semantic for the expression *satisfactory covering subset* adopted in this thesis is explained. Then, the role of each one of the three unions is detailed. It is to be noticed that the union of subsets having the satisfactory covering property for a set represents also a satisfactory covering subset of that set.

$$\begin{aligned} REF &= \bigcup_{i=1}^m C_i^{ref} \\ PARAM &= \bigcup_{i=1}^m C_i^{param} \\ TEST &= \bigcup_{i=1}^m C_i^{test} \end{aligned} \quad (7)$$

4.2.6.1. Satisfactory Covering Subsets

For the work presented in this thesis, a *satisfactory covering subset* represents a subset of data that preserves (with a given order of magnitude) the distribution of the data associated with the problem. Selecting the elements that compose a satisfactory covering subset for a given data set can be costly. Therefore, it is more convenient to use selection methods that provide convenient approximations for satisfactory covering subsets. Such a method is proposed in the following.

Let us consider a given finite data set A that contains r points in a multidimensional space. First, the maximum distance, max , between two elements is computed. During this computation a pair of elements, (a,b) , with maximum distance between them is memorized. Then, one of the elements, let it be a , is considered as the centre of s hyperspheres, S_i , $i=1, \dots, s$. The user must provide the s value. Each one of the S_i hyperspheres has a radius equal to

$$r_i = i \frac{max}{s}, \quad i = 1, \dots, s \quad (8)$$

The next step is to consider the partition induced by the next subsets,

$$\begin{aligned} P_0 &= \{a \in A / a \text{ inside } S_1\} \\ P_j &= \{a \in A / a \text{ inside } S_{j+1} - S_j\}, \quad j = 1, \dots, s-1 \end{aligned} \quad (9)$$

The cardinal of the subset that approximates the satisfactory covering subset is set to a previous given percent t of elements from A . The distribution of elements from A in the partition elements P_0, \dots, P_{s-1} is not equal. This distribution is taken into account when distributing the percent t among the partition members. Each partition member P_j , $j=1, \dots, s-1$, will be allocated a number of p_j elements. The approximation subset is composed by randomly selecting p_j elements from the P_j subset, $j=1, \dots, s-1$.

4.2.6.2. Reference Patterns Set (REF)

The point-to-set similarity measures are defined for the representative subsets C_i^{ref} , $i=1, \dots, m$. Therefore, when using a single point-to-set similarity measure, the fuzzy membership functions are computed as

$$\mu_i(u) = \frac{r(u, C_i^{ref})}{r(u, C)} \quad (10)$$

4.2.6.3. Parameters Tuning Set (PARAM)

The shape of the membership functions μ_i , associated to the fuzzy sets F_{uzz_i} , depends not only on the representative subset C_i^{ref} , but also on the value of the β_i parameter, $i=1, \dots, m$. The algorithm for tuning the parameters β_i , $i=1, \dots, m$, of the classifier represents a search process in an m -dimensional space for the parameter vector $(\beta_1, \beta_2, \dots, \beta_m)$ that meets, for each category, the maximal correct classification criterion and the minimal misclassification criterion. In order to perform this search, different methodologies may be used, i.e. genetic algorithms (Bocaniala *et al.*, 2003), hill-climbing (Bocaniala and Sa da Costa, 2004a) and particle swarm optimisation (PSO) (Bocaniala and Sa da Costa, 2004b). In practice, the PSO methodology proved to be the fastest.

The search for optimal parameters when using genetic algorithms and hill-climbing may be accelerated by using an *optimised initial population* (Sa da Costa *et al.*, 2003). An optimised initial population can be obtained by performing an iterative search that starts with an individual whose parameters have very small values. Then, at each next step, the values of the parameters will be increased/decreased so that the fitness of the obtained individual, i.e., the classifier performance, increases.

4.2.6.4. Testing Set (TEST)

The performance of the classifier is measured according to its generalization capabilities when applied on the *TEST* set. It is to be noticed that the *TEST* set contains data that were not presented before at the input of the classifier and that is representative for the whole data set C . The practice showed that the performance of the classifier may improve if the testing is performed after adding the data in the *PARAM* set to the *REF* set.

4.3. Detailed Analysis of Faults in the Case Study

The DAMADICS benchmark (<http://www.eng.hull.ac.uk/research/control/damadics1.htm>) is concerned with fault diagnosis of a valve intended to supply water to a steam generator boiler. The valve is used as part of the process at sugar factory Cukrownia Lublin S.A., Poland. It is made up of three parts: a valve body, a spring-and-diaphragm pneumatic actuator and a positioner (Figure 4.8). The valve body is the equipment that sets the flow through the pipe system. The flow is proportional to the minimum flow area inside the valve (2), which, in turn, is proportional to the position of a rod (5). The spring-and-diaphragm actuator determines the position of this rod. The spring-and-diaphragm actuator is composed of a rod, which at one end

is connected to the valve body and the other end has a plate, which is placed inside a pneumatic chamber (8). The plate is connected to the walls of the chamber by a flexible diaphragm. This assembly is supported by a spring. The position of the rod is proportional to the pressure inside the chamber, which is determined by the positioner. The positioner is basically a control element. It receives three signals: a measurement of the position of the rod (x), a reference signal for the position of the rod (CV) and a pneumatic signal from a compressed air circuit in the plant. The positioner returns an airflow signal, which is determined by a classic feedback control loop of the rod position. The airflow signal changes the pressure inside the chamber.

There are several sensors included in the system that measure the variables that influence the system, namely, the upstream and downstream water pressures, the water temperature, the position of the rod (x) and the flow through the valve (F). These measurements are intended for controlling the process but they can also be used for FDI purposes. This means that the implementation of this sort of system will not imply additional hardware. The first three measurements, as well as the control value (CV), may be seen as the inputs to the system whilst the latter two may be seen as its outputs. The two output values, the sensor for measuring the position of the rod (x) and the sensor for measuring the water flow through the valve (F), provide variables that contain information relative to the faulty behaviours.

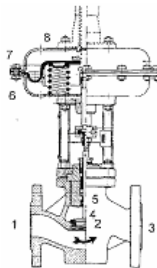


Figure 4.8. The valve studied by DAMADICS benchmark.

The sensor measurements corresponding to some faults cannot be obtained directly from the real process as the occurrence of these faults may have disastrous consequences on the system. Therefore, the valve needed to be extensively modelled using the physical laws that govern its behaviour (Louro, 2003; Sa da Costa and Louro, 2003). The MATLAB/SIMULINK model obtained may be used to simulate any faulty behaviour.

The faults in the benchmark have been simulated for 20 different values of fault strength, uniformly distributed between 5% and 100%, and different input values for the reference signal. The previous set of fault strengths represents a good approximation of all possible faulty situations involving the faults in the benchmark. All faults have been simulated two times for all their fault strengths. The simulation lasted for 70 seconds the first time and for 20 seconds the second time. The fault has been introduced at the 50th second the first time and at the 10th the second time. The data obtained during the first simulation have been used to

design the classifier, i.e., 50% for the *REF* set and 50% for the *PARAM* set. The data obtained during the second simulation have been used as the *TEST* set. For the second round of simulation a shorter time has been chosen, i.e., the fault is introduced in the system for only 10 seconds, as good fault diagnosis methodologies need to have very short time intervals for detection and isolation of abrupt faults.

The input to the simulation is taken from real data collected at the plant. This method provides more realistic conditions for generating the behaviour of the system while undergoing a fault. It also makes the FDI task more difficult because the real data input causes the system to feature the same noise conditions as those in the real plant.

The valve is affected by a total of 19 faults that may have abrupt and/or incipient behaviour (Table 4.1). In this chapter only the abrupt manifestation of the faults has been considered. The large majority of faults, 14 out of 19, manifest an abrupt behaviour.

Table 4.1. The set of faults considered in DAMADICS benchmark

Fault	Description	Abrupt behavior			Incipient behaviour
		small	medium	big	
F1	Valve clogging	x	x	x	
F2	Valve plug or valve seat sedimentation			x	x
F3	Valve plug or valve seat erosion				x
F4	Increase of valve or bushing friction				x
F5	External leakage (leaky bushing, covers, terminals)				x
F6	Internal leakage (valve tightness)				x
F7	Medium evaporation or critical flow	x	x	x	
F8	Twisted servo-motor's piston rod	x	x	x	
F9	Servomotor's housing or terminals tightness				x
F10	Servomotor's diaphragm perforation	x	x	x	
F11	Servomotor's spring fault			x	x
F12	Electro-pneumatic transducer fault	x	x	x	
F13	Rod displacement sensor fault	x	x	x	x
F14	Pressure sensor fault	x	x	x	
F15	Positioner feedback fault			x	
F16	Positioner supply pressure drop	x	x	x	
F17	Unexpected pressure change across the valve			x	x
F18	Fully or partly opened bypass valve	x	x	x	x
F19	Flow rate sensor fault	x	x	x	

As mentioned in the introduction of this chapter, the sensor that measures the rod position (x) and the sensor that measures the flow (F) provide variables that contain information relative to the faults. The difference dP between the upstream pressure measurement (P_1) and the downstream pressure measurement (P_2) is also considered (besides x and F) as it permits to differentiate *F17* from the other faults. For the rest of the faults, the previous difference always has negligible values (close to zero).

The effects of three out of the 14 abrupt faults on these three sensor measurements are not distinguishable from the normal behaviour (N), $\{F8, F12,$

$F14$ }. Therefore, in the following, these cases are not studied. They can be dealt with if further sensors are added to the system. There can be distinguished three groups of faults, $\{F2, F19\}$, $\{F7, F10\}$, and $\{F11, F15, F16\}$, for which exists a strong similarity between their effects on the measurements, i.e., large overlapping. There is also noncritical overlapping between the groups of faults $\{F1, F7\}$ and $\{F13, F18\}$.

4.4. Results of Fault Diagnosis Using the Fuzzy Classifier

The previous section indicated the three sensor measurements, x , F and dP , that provide the best distinction among the faults. In order to provide the classifier with information on the dynamics of the system, the state of the system is described using the aggregate of these values over a time window of 5 time-steps. More precisely, the state of the system represents a point in a 15-dimensional space, $(x_{t-4}, \dots, x_t, F_{t-4}, \dots, F_t, dP_{t-4}, \dots, dP_t)$, where t is the time instance when the system state is recorded. The classifier performs detection and isolation in one single step. If the classifier outputs the same fault label for two consecutive states then the system is diagnosed as being affected by that fault.

The classifier employed in this chapter is built using a hybrid approach based on Euclidean distance and Pearson correlation. Pearson correlation allows the trends in the x and F signals to provide supplementary separation between different faults. As mentioned before, a point in a 15-dimensional space describes the system state, i.e. the record over 5 consecutive time-steps for dP , x and F values. Therefore, the point has associated two vectors that represent the trend for x and F signals over the 5 time-step window. Three point-to-set similarity measures are used, based on the three similarity measures induced by the Euclidean distance (r_E), Pearson correlation for x (r_{P_x}), and Pearson correlation for F (r_{P_F}), respectively. The β parameters are applied only to the point-to-point similarity measure based on the Euclidean distance. If the β parameters are applied only to one of the point-to-point similarity measures used, then all other point-to-set similarity measures will be computed for the neighbourhood defined by these β parameters. The point-to-set similarity measures corresponding to each of the two Pearson correlations are given by Eq. 11, where p_x and p_F stand for the point-to-point similarities based on Pearson correlation for x and F , respectively. Finally, the fuzzy membership functions represent a combination of the three point-to-set similarity measures (Eq. 12). The terms σ , τ and ζ weight the contribution of each point-to-set similarity measure to the overall value. The search process for the optimal β parameters may be extended to also tune the values of these terms.

$$\begin{aligned}
 r_{P_x}(u, C_i) &= \sum_{\substack{\text{all } v \text{ in the} \\ \text{neighbourhood} \\ \text{defined by } \beta_i}} (2 - p_x(u, v)) \\
 r_{P_F}(u, C_i) &= \sum_{\substack{\text{all } v \text{ in the} \\ \text{neighbourhood} \\ \text{defined by } \beta_i}} (2 - p_F(u, v))
 \end{aligned} \tag{11}$$

$$\mu_i(u) = \frac{\sigma * \frac{r_E(u, C_i)}{r_E(u, C)} + \tau * \frac{r_{P-x}(u, C_i)}{r_{P-x}(u, C)} + \xi * \frac{r_{P-F}(u, C_i)}{r_{P-F}(u, C)}}{\sigma + \tau + \xi} \quad (12)$$

The process of fault detection and isolation will follow the next two steps. First, only one category per fault is considered, containing all the points associated with all possible fault strengths. Second, more than one category for one fault is considered. These categories are formed by allowing for single fault strengths or groups of fault strengths to form distinct categories (Bocaniala *et al.*, 2004). The second step is taken in order to increase even more (if possible) the isolation capabilities of the classifier until distinguishing between different fault strengths.

For the first step, one category per fault is considered and a classifier is built for this particular set of categories. The isolation matrix obtained is shown in Table 4.2. The normal state (N) is separable/well-classified from the faulty states in proportion of 99.60%. The comment “*not visible*” stands for situations when the effects of the corresponding fault strengths are not visible. Analysing the content of Table 4.2 the following facts may be deduced. The classifier correctly recognizes the five groups of overlapping faults mentioned in Section 4.3. Notice that the large overlapping between $F11$, $F15$ and $F16$ is almost completely solved. Notice also that in the case of faults $F1$, $F10$, $F18$ and $F19$, the effects of the small fault strengths are not distinguishable from the normal state. The previous analysis proves the high accuracy with which the classifier is able to delimit the areas corresponding to different categories, and the fine precision of discrimination inside overlapping areas. However, the content of Table 4.2 raises questions like the next one: if the classifier outputs the label $F15$, then is this fault in the system really $F15$ (and if it is which fault strength does it have), or is it fault strength 95% of $F11$, or is it fault strength 75% of $F16$? The second step of the process of detection and isolation investigates the answers to questions like the previous one, i.e., tries to improve the isolation.

For the second step, more than one category per fault is considered. These categories are formed by allowing for single fault strengths or groups of fault strengths to a distinct category (Bocaniala *et al.*, 2004). As will be seen, this refinement increases the isolation between different faults and between different fault strengths of the same fault. The effects of the refinement are studied considering the faults grouped according to the overlapping between them, i.e., $\{F1, F7\}$, $\{F2, F19\}$, $\{F7, F10\}$, $\{F11, F15, F16\}$, $\{F13, F18\}$ and $\{F17\}$. For each group of faults the next analysis is performed. First, for each fault, the clustering into groups of fault strengths is found by considering the fault strengths as separate categories and building the corresponding classifier. For each fault, the identified groups of fault strengths represent the new set of categories per fault. Second, using the previous sets of categories per fault, another classifier is built in order to check the isolation properties. The result of these analyses is presented in Tables 4.3 to 4.7. The notation used is $FiFSj$, where i and j respectively stand for the fault label and fault strength (given as a number between 0 and 100). The labelling convention for the clusters formed by more than one fault strength is to use the label corresponding to the smallest fault strength in the group, i.e., the two clusters for $F2$ are labelled $F2FS70$ and respectively $F2FS80$.

Table 4.2. The isolation matrix for the case when only one category per fault is considered

	1	2	3	4	5	6	7	8	9	10	11	12	13	14	15	16	17	18	19	20	
	5%	10%	15%	20%	25%	30%	35%	40%	45%	50%	55%	60%	65%	70%	75%	80%	85%	90%	95%	100%	
F1	[-	-	-	N	-	-	-	-	-	-	-	-	-	F1	-	-	-	-	-	F7
F2	[-	-	-	not considered in the benchmark					-	-	-	-	-	F2	F2	F19	F2	F2	F19	F2
F7	[-	-	-	-	-	-	-	-	-	-	-	-	-	-	-	-	-	-	-	-
F10	[-	-	-	N	-	-	-	-	F10	F10	-	-	-	-	-	-	-	-	-	F7
F11	[-	-	-	not considered in the benchmark					-	-	-	-	-	-	-	-	-	-	-	-
F13	F18	F18	F13	F18	[-	-	-	-	-	-	-	-	-	-	-	-	-	-	-	-
F15	[-	-	-	not considered in the benchmark					-	-	-	-	-	F15	F15	F15	-	-	-	-
F16	[-	-	-	-	-	-	N	-	-	-	-	-	-	-	-	-	-	-	-	-
F17	[-	-	-	not considered in the benchmark					-	-	-	-	-	-	-	-	-	-	-	-
F18	N	[-	-	F13	-	-	-	-	-	-	-	-	-	-	-	-	-	-	-	-
F19	N	N	[F19	-	F2	[-	-	-	-	-	-	-	-	-	-	-	-	-	-

Table 4.3. The isolation matrix for the group of faults {F1, F7} in case when more than one category per fault is considered

	1	2	3	4	5	6	7	8	9	10	11	12	13	14	15	16	17	18	19	20	
	5%	10%	15%	20%	25%	30%	35%	40%	45%	50%	55%	60%	65%	70%	75%	80%	85%	90%	95%	100%	
F1	[-	-	-	N	-	-	-	-	F1FS45	F1FS50	F1FS55	F1FS60	F1FS65	F1FS70	F1FS75	F1FS80	F1FS85	F1FS90	F1FS95	F7
F7	[-	-	-	-	-	-	-	-	-	-	F7	-	-	-	-	-	-	-	-	-

Table 4.4. The isolation matrix for the group of faults {F2, F19} in case when more than one category per fault is considered

	1	2	3	4	5	6	7	8	9	10	11	12	13	14	15	16	17	18	19	20		
	5%	10%	15%	20%	25%	30%	35%	40%	45%	50%	55%	60%	65%	70%	75%	80%	85%	90%	95%	100%		
F2	[-	-	-	not considered in the benchmark					-	-	-	-	-	-	F19FS15	F2FS70	F19FS30	F2FS80	F2FS70	F19FS30	F2FS80
F19	N	N	[-	F19FS15	-	-	-	-	-	-	-	-	-	-	-	-	-	-	-	-	
						F19FS30	[-	-	-	-	F19FS35	-	-	-	-	F19FS80	[-	-	F19FS35	

Table 4.5. The isolation matrix for the group of faults {F7, F10} in case when more than one category per fault is considered

	1	2	3	4	5	6	7	8	9	10	11	12	13	14	15	16	17	18	19	20	
	5%	10%	15%	20%	25%	30%	35%	40%	45%	50%	55%	60%	65%	70%	75%	80%	85%	90%	95%	100%	
F7	[-	-	-	-	-	-	-	-	-	-	-	-	-	-	-	-	-	-	-	-
F10	[-	-	-	N	-	-	-	-	F10FS45	F10FS45	-	-	-	F10FS70	F10FS70	[-	-	-	F7

Table 4.6. The isolation matrix for the group of faults {F13, F18} in case when more than one category per fault is considered

	1	2	3	4	5	6	7	8	9	10	11	12	13	14	15	16	17	18	19	20
	5%	10%	15%	20%	25%	30%	35%	40%	45%	50%	55%	60%	65%	70%	75%	80%	85%	90%	95%	100%
F13	F13FS5	F18FS10	F13FS5	F18FS10	F13FS5	F18FS10	F13FS5	F13FS5	[-	-	-	-	-	-	-	-	-	-	-
F18	N	F18FS10	F13FS5	[-	-	-	F18FS10	-	-	-	-	-	-	-	F18FS40	-	-	-	-

Table 4.7. The isolation matrix for the group of faults {F11, F15, F16} in case when more than one category per fault is considered

	1	2	3	4	5	6	7	8	9	10	11	12	13	14	15	16	17	18	19	20	
	5%	10%	15%	20%	25%	30%	35%	40%	45%	50%	55%	60%	65%	70%	75%	80%	85%	90%	95%	100%	
F11	[-	-	-	not considered in the benchmark					-	-	-	-	-	-	-	-	-	-	-	-
F15	[-	-	-	not considered in the benchmark					-	-	-	-	-	-	F15FS70	F15FS75	F15FS80	-	-	-
F16	[-	-	-	-	-	-	N	-	-	-	-	-	-	-	-	-	-	-	-	

Notice that the isolation results have improved radically. For instance, the medium and large fault strengths of *F19*, 40-100%, are separated from the small ones, 5-35%; while misclassification of *F19* with *F2* occurs only for the small strengths of *F19*. The overlapping between faults *F13* and *F18* occurs now only between small fault strengths, i.e., between 5% and 30% for *F13* and 10% and 35%

for *F18*. The medium and large strengths of both faults are now perfectly separated from each other.

4.5. Conclusions

This chapter presented a novel fuzzy classification methodology applied to fault diagnosis. There are three main directions of applying fuzzy classifiers to fault diagnosis: neuro-fuzzy classifiers, classifiers based on collections of fuzzy rules, and classifiers based on collections of fuzzy subsets. The fuzzy classification methodology described in this chapter follows the last direction. The main property of this methodology is the large accuracy with which it learns the topological structure of the symptoms space. The fuzzy subsets built by the classifier approximate with a very small error the areas in the symptoms space corresponding to different categories. Its accuracy also manifests through handling with fine precision the discrimination inside overlapping areas.

The technique of building fuzzy subsets used with the contributed methodology is based on the work of Baker (1978). The original contributions are (i) the use of different (dedicated) β parameters for different categories to express the point-to-point similarity in order to increase the performance of the classifier, (ii) developing the idea acknowledged by Baker (1978) that the use of fuzzy subsets induced by multiple point-to-set similarity measures may increase the performance of the classifier, (iii) for the case study, the use of a 5 time-step time window that allows information on the system dynamics to be used with the classifier, and (iv) also for the case study, the improvement in the isolation capability by allowing single fault strengths or groups of fault strengths to form distinct categories used with the classifier.

Future research on the fuzzy classification methodology needs to concentrate on obtaining a computational complexity of both design and test phase that is small enough to make the classifier suitable for application to fault diagnosis of real systems. The computational complexity of the design phase has already been significantly reduced by using the particle swarm optimisation technique (Bocaniala and Sa da Costa, 2004a; 2004b). Also, it has been observed in practice that the classifier generalises reasonably well even for small dimensions of the *REF* and *PARAM* sets (Bocaniala, 2003). Or, the computational complexity of both the design and test phase depends heavily on the sizes of these two sets. This leads to the conclusion that a technique might be found so that the sizes of these two sets drop substantially and so that the performance of the classifier stays at least the same. An answer might be found by studying the kernel methods (Shawe-Taylor and Cristianni, 2004).

Acknowledgements

This work was partially supported by the European Commission's FP5 Research Training Network Program – Project “DAMADICS – Development and

Application of Methods for Actuator Diagnosis in Industrial Control Systems,” and by Fundação para a Ciência e a Tecnologia, Minister of Science, Innovation and Technology, Portugal, grant number SFRH/BD/18651/2004

References

1. Arifon V and Palade V (2005) Human-like fault diagnosis using a neural network implementation of plausibility and relevance. *Neural Computing & Applications* 14(2):149-165.
2. Baker E (1978) Cluster analysis by optimal decomposition of induced fuzzy sets (PhD thesis). Delftse Universitaire Pres, Delft, Holland.
3. Bocaniala CD (2003) Tehnici de inteligență artificială aplicate în diagnoza defectelor: Aplicații ale tehnicilor de clasificare (Technical Research Report within doctoral training). University “Dunarea de Jos” of Galati, Romania, 2003. (available in English for download at www.gcar.dem.ist.utl.pt/pessoal/cosmin/index.htm)
4. Bocaniala CD and Sa da Costa J (2004a) Tuning the Parameters of a Fuzzy Classifier for Fault Diagnosis. Hill-Climbing vs. Genetic Algorithms. In: Proceedings of the Sixth Portuguese Conference on Automatic Control (CONTROLO 2004), 7-9 June, Faro, Portugal, pp. 349-354.
5. Bocaniala CD and Sa da Costa J (2004b) Tuning the Parameters of a Fuzzy Classifier for Fault Diagnosis. Particle Swarm Optimization vs. Genetic Algorithms. In: Proceedings of the 1st International Conference on Informatics in Control, Automation and Robotics ICINCO 2004, 25-28 August, Setubal, Portugal, vol. 1, pp. 157-162.
6. Bocaniala CD, Sa da Costa J and Louro R (2003) A Fuzzy Classification Solution for Fault Diagnosis of Valve Actuators. In: Proceedings of 7th International Conference on Knowledge-Based Intelligent Information & Engineering Systems, Oxford, UK, September 3-5, Part I, pp. 741-747, LNAI Series, Springer-Verlag, Heidelberg, Germany.
7. Bocaniala CD, Sa da Costa J and Palade V (2004) A Novel Fuzzy Classification Solution for Fault Diagnosis. *International Journal of Fuzzy and Intelligent Systems* 15(3-4): 195-206.
8. Bocaniala CD, Sa da Costa J and Palade V (2005) Fuzzy-based refinement of the fault diagnosis task in industrial devices. *International Journal of Intelligent Manufacturing* 16(6): 599-614.
9. Boudaoud N and Masson M (1996) The diagnosis of technological system: on-line fuzzy clustering using gradual confirmation of prototypes. In: Proceedings of CESA'96, France.
10. Boudaoud N and Masson M (2000) Diagnosis of transient states using pattern recognition approach. *JESA – European Journal of Automation* 3: 689-708.
11. Calado JMG, Korbicz J, Patan K, Patton RJ and Sa da Costa JMG (2001) Soft Computing Approaches to Fault Diagnosis for Dynamic Systems. *European Journal of Control* 7: 248-286.

12. Chen J and Patton RJ (1999) Robust Model-Based Fault Diagnosis for Dynamic Systems. Asian Studies in Computer Science and Information Science, Kluwer Academic Publishers, Boston.
13. Duda RO and Hart PE (1973) Pattern classification and scene analysis. John Wiley & Sons, New York.
14. European Community's FP5, Research Training Network DAMADICS Project, <http://www.eng.hull.ac.uk/research/control/damadics1.htm>.
15. Frank PM (1996) Analytical and qualitative model-based fault diagnosis – a survey and some new results. European Journal of Control 2: 6-28.
16. Koscielny JM, Sedziak D and Zackroczynsky K (1999) Fuzzy-logic fault isolation in large-scale systems. International Journal of Applied Mathematics and Computer Science 9(3): 637-652.
17. Leonhardt S and Ayoubi M (1997) Methods of fault diagnosis. Control Engineering Practice 5(5): 683-692.
18. Louro R (2003) Fault Diagnosis of an Industrial Actuator Valve (MSc dissertation). Instituto Superior Técnico, Lisbon, Portugal.
19. Palade V, Patton RJ, Uppal FJ, Quevedo J and Daley S (2002) Fault Diagnosis of An Industrial Gas Turbine Using Neuro-Fuzzy Methods. In: Proceedings of the 15th IFAC World Congress, 21–26 July, Barcelona, pp. 2477–2482.
20. Sa da Costa J, Bocaniala CD and Louro R (2003) A Fuzzy Classifier for Fault Diagnosis of Valve Actuators. In: Proceedings of IEEE Conference on Control Applications CCA 2003, Istanbul, Turkey.
21. Sa da Costa J and Louro R (2003) Modelling and simulation of an industrial actuator valve for fault diagnosis benchmark. In: Proceedings of the Fourth International Symposium on Mathematical Modelling, Vienna, pp. 1212-1221, Agersin-Verlag.
22. Shawe-Taylor J and Cristianini N (2004) Kernel methods for pattern analysis. Cambridge University Press.
23. Simpson PK (1993) Fuzzy min-max neural networks – Part 2: Clustering. IEEE Transactions on Fuzzy Systems 1(1): 32-45.
24. Uppal FJ, Patton RJ and Palade V (2002) Neuro-Fuzzy Based Fault Diagnosis Applied to an Electro-Pneumatic Valve. In: Proceedings of the 15th IFAC World Congress, 21–26 July, Barcelona, Spain, pp. 2483-2488.
25. Weisstein EW (1999) Correlation Coefficient. From MathWorld--A Wolfram Web Resource, <http://mathworld.wolfram.com/CorrelationCoefficient.html>.